Size-Dependent Ultrafast Magnetization Dynamics in Iron Oxide (Fe$_3$O$_4$) Nanocrystals

Chih-Hao Hsia, Tai-Yen Chen, and Dong Hee Son*

Department of Chemistry, Texas A&M University, College Station, Texas 77842

ABSTRACT

Optically induced ultrafast demagnetization and its recovery in superparamagnetic colloidal iron oxide (Fe$_3$O$_4$) nanocrystals have been investigated via time-resolved Faraday rotation measurements. Optical excitation with near-infrared laser pulse resulted in ultrafast demagnetization in ∼100 fs via the destruction of ferrimagnetic ordering. The degree of demagnetization increased with the excitation density, and the complete demagnetization reached at ∼10% excitation density. The magnetization recovered on two time scales, several picoseconds and hundreds of picoseconds, which can be associated with the initial reestablishment of the ferrimagnetic ordering and the electronic relaxation back to the ground state, respectively. The amplitude of the slower recovery component increased with the size of the nanocrystals, suggesting the size-dependent ferrimagnetic ordering throughout the volume of the nanocrystal.

Ultrafast dynamics of the magnetization in magnetic materials attracted a great deal of attention in recent years.[1,2] In particular, modification of the magnetization on subpicosecond time scales using femtosecond optical pulses in ferro- and antiferromagnetic materials has been the subject of heated debates and active investigations.[3−8] Because the ultrashort optical excitation could manipulate the magnetization on the time scales much faster than the typical spin−lattice relaxation time (>100 ps), a significant effort has been made to understand the microscopic mechanism. During the past decade, various mechanisms including both thermal and nonthermal pathways were proposed to explain the optically induced ultrafast demagnetization, magnetization, and spin switching.[9−11]

From a practical point of view, the ability to control the ultrafast magnetization is very important in applications such as spintronics and magnetic data storage devices.[12,13] Due to the continuing demand for higher-speed and larger-capacity devices, ultrafast magnetization dynamics in nanometer scale magnetic structures also gained much attention.[14] Earlier efforts to investigate the ultrafast dynamics of the magnetization in magnetic nanostructures mainly focused on thin film structures with one-dimensional spatial confinement or mesoscopic structures. On the other hand, magnetic structures with three-dimensional spatial confinement received much less attention,[15,16] while the finite-size effect in nanometer length scale could be more systematically investigated. In this respect, colloidal magnetic nanocrystals

are very useful for investigating the ultrafast dynamics of the magnetization in three-dimensionally confined magnetic structures. The merits of colloidal nanocrystals in the study of finite-size effect on various ultrafast dynamic processes were previously well demonstrated in semiconductors nanocrystals,[17,18] where the methods of size and shape control are highly developed.

In this letter, we report the femtosecond time-resolved studies on the optically induced ultrafast magnetization dynamics in size-controlled superparamagnetic Fe$_3$O$_4$ nanocrystals as a model system for the three-dimensionally confined magnetic nanostructures. Linearly polarized femtosecond optical pulses at 780 nm excited the weak absorption originating from the intervalence charge-transfer transition between Fe^{3+} and Fe^{2+} ions. The excitation resulted in an instantaneous decrease of Faraday rotation, indicating ultrafast photoinduced demagnetization. The Faraday rotation recovered on multiple time scales ranging from a few to hundreds of picoseconds. Here, we investigated how the dynamics of the ultrafast demagnetization and its recovery are affected by the density of the optical excitation and the size of the nanocrystals.

Spherical Fe$_3$O$_4$ nanocrystals of three different sizes (4.5, 7.5, and 10 nm in diameter) were synthesized following the previously reported procedure.[19] Fe$_3$O$_4$ nanocrystals were suspended in cyclohexane for all the measurements of this study. While bulk Fe$_3$O$_4$ is ferrimagnetic, nanocrystals in these size ranges are superparamagnetic at room temperature.[20] Figure 1,panels a and b, shows the typical optical absorption spectrum and transmission electron microscopy

* To whom correspondence should be addressed. E-mail: dhson@ mail.chem.tamu.edu. Phone: 979-458-2990.
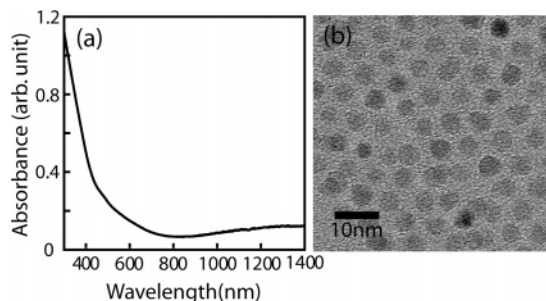
Figure 1. (a) UV−vis absorption spectrum of Fe_3O_4 nanocrystals. (b) TEM image of 4.5 nm Fe_3O_4 nanocrystals.
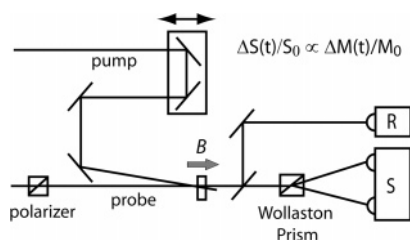
Figure 2. Schematic diagram of the time-resolved Faraday rotation measurement. The external magnetic field (B) was provided by a pair of permanent magnets, whose polarity was set either parallel or perpendicular to the direction of the probe light.

(TEM) image of Fe_3O_4 nanocrystals, respectively. The visible absorption is primarily due to the mixture of the ligand field transition and charge-transfer transition, while near-infrared absorption is assigned to the intervalence charge-transfer transition between the metal ions.[21] The excitation fluence was varied in the range of $15-61$ mJ/cm^2 resulting in the corresponding average excitation density in the range of $3-12\%$. The approximate average excitation density was estimated from the concentration of the nanocrystals and the absorbed excitation pulse energy. The concentration of nanocrystals was kept low to maintain the average interparticle distance much larger than the size of the nanocrystal (e.g., factor of ~10). Dipolar interaction between the nanocrystals is insignificant at these concentrations and should not affect the dynamics of the magnetization.[22]

Time-dependent magnetization of the photoexcited Fe_3O_4 nanocrystals was monitored by time-resolved Faraday rotation measurements. Faraday rotation is proportional to $\vec{M}(t)\cdot\vec{k}$, where $\vec{M}(t)$ and $\vec{k}$ are the magnetization vector of the nanocrystal and wavevector of the probe light, respectively.[23] Due to the high temporal resolution, time-resolved Faraday rotation and the related technique of magneto-optic Kerr effect have been widely utilized in the study of the ultrafast magnetic responses.[3,11,24−26] A schematic diagram of the experimental setup is shown in Figure 2. Linearly polarized pump pulses (780 nm, 60 fs, 3 kHz) excited the free-streaming jet (400 μm thick) of nanocrystals at room temperature and under the external magnetic field of 0.35 T. The sample solution was circulated as a jet form to prevent potential sample damage and accumulated thermal effects due to the repeated exposure of the same sample area to the pump pulses. The linearly polarized probe pulses at 620 or 900 nm, derived from white light continuum, were used to monitor the time-dependent Faraday rotation of the photo-
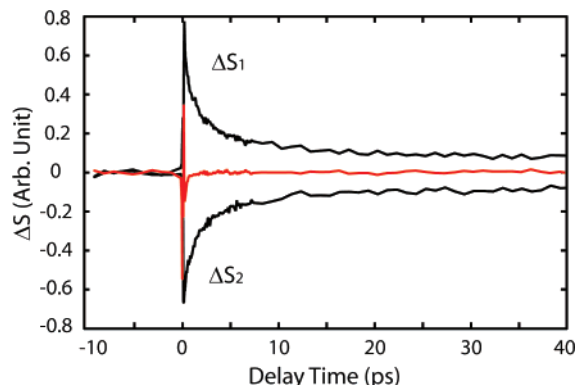
Figure 3. Time-resolved Faraday rotation of Fe_3O_4 nanocrystals (7.5 nm). ΔS_1 and ΔS_2 were obtained under Faraday geometry with the two opposite polarities of the external magnetic field. For these two curves, the signal obtained without the external magnetic field was subtracted. The red curve is obtained under Voigt geometry.

excited samples. Combination of a Wollaston prism and a balanced photodiode pair was used to measure the Faraday rotation, which is proportional to the output signal from the balanced photodiode normalized to the transmitted probe intensity, S/R, for a small rotation angle. Fractional changes of magnetization induced by the optical excitation was obtained by measuring $\Delta S/S_0$, where $\Delta S = [S(\text{pump on}) - S(\text{pump off})]/R$ and $S_0 = S(\text{pump off})/R$, respectively. The measured signal $\Delta S/S_0$ in this study reflects in principle the complex Faraday rotation with contributions of circular birefringence and dichroism, both of which are linear to the magnetization.[27]

Figure 3 shows the representative pump−probe Faraday rotation data of 7.5 nm Fe_3O_4 nanocrystals under Voigt and Faraday geometries. The probe light propagates in the direction perpendicular and parallel to the external magnetic field for Voigt and Faraday geometry, respectively. Under the Voigt geometry, Faraday rotation exhibits essentially no dynamic response except a spike near zero time delay originating from optical Kerr effect. Under the Faraday geometry, an immediate decrease of Faraday rotation was observed with the subsequent recovery of the signal on two distinct time scales. The opposite polarity of the external magnetic field yielded signals with the opposite sign (ΔS_1 and ΔS_2), because the Faraday effect is odd with respect to the magnetic field.[27] To remove any potential nonmagnetic feature in the dynamics, the difference between ΔS_1 and ΔS_2 were taken to obtain the time-dependent magnetization throughout the measurements.

No signature of a precession of the magnetization vector was observed up to 3 ns of delay time for both Faraday and Voigt geometries. The lack of precessional signature may be due to negligible photoinduced reorientation of the magnetization or critical damping of the precession.[15,28] If the reorientation of the magnetization can be ignored, the fractional Faraday rotation ($\Delta S/S_0$) can be interpreted as the fractional changes in the amplitude of the magnetization ($\Delta M/M_0$) in the nanocrystals.

In Figure 4, pump−probe transient absorption (ΔOD) and magnetization data ($\Delta M/M_0$) are shown together to compare
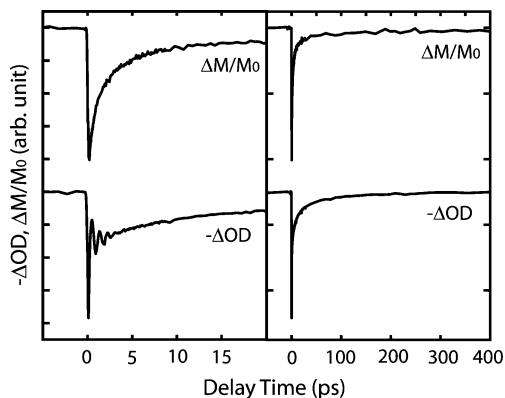
Figure 4. Comparison of the transient absorption ($-\Delta OD$) and magnetization ($\Delta M/M_0$). The left and right panels display the same data set in different time windows.

the electronic and magnetic responses to the ultrafast optical excitation. For an easy comparison of the dynamics, the sign of the transient absorption data is reversed in the figure. The transient absorption data exhibit pump-induced absorption in the broad range of visible and near-infrared probe wavelengths, which decays on multiple time scales with exponential time constants of $\tau = \sim 20$ and ~ 200 ps. The time scales of the dynamics were weakly dependent on the probe wavelengths within the range $550-900$ nm, while the amplitude varied with the wavelength. (See Supporting Information) The oscillations at early delay times are due to the coherent acoustic phonon. On the other hand, dynamics of magnetization exhibits noticeable differences from the transient absorption at delay times earlier than 20 ps, while they exhibit comparable dynamics on much slower time scales. The initial recovery of the magnetization ($\Delta M/M_0$) following the ultrafast demagnetization occurs on a few picoseconds time scale and carries a larger fraction of recovery amplitude. This component of the dynamics is absent in the transient absorption data. The oscillatory features are not observable unlike in transient absorption data indicating that the coherent lattice motion does not have a measurable effect on $\Delta M/M_0$ in this study. The slower recovery component of the magnetization occurs with exponential time constants of $\tau = \sim 200$ ps, which are similar to the transient absorption data. The measured $\Delta M/M_0$ is independent of the probe wavelength exhibiting essentially identical dynamics at 620 and 900 nm. (See Supporting Information)

The immediate decrease of $\Delta M/M_0$ following the optical excitation in ~ 100 fs is assigned to the ultrafast demagnetization by the destruction of the ferrimagnetic ordering upon the optical excitation. Optically induced demagnetization on subpicosecond time scale was previously observed on the surface of many ferro- and ferrimagnetic materials,[3,29] although the exact mechanism has been debated for many years. Demagnetization by the equilibration of the laser-heated lattice and spin system via usual spin−lattice interaction is unlikely because the time scale for such process typically exceeds 100 ps. Various mechanisms of optically induced ultrafast demagnetization were proposed such as spin-flip electron scattering, femtosecond spin−lattice re-
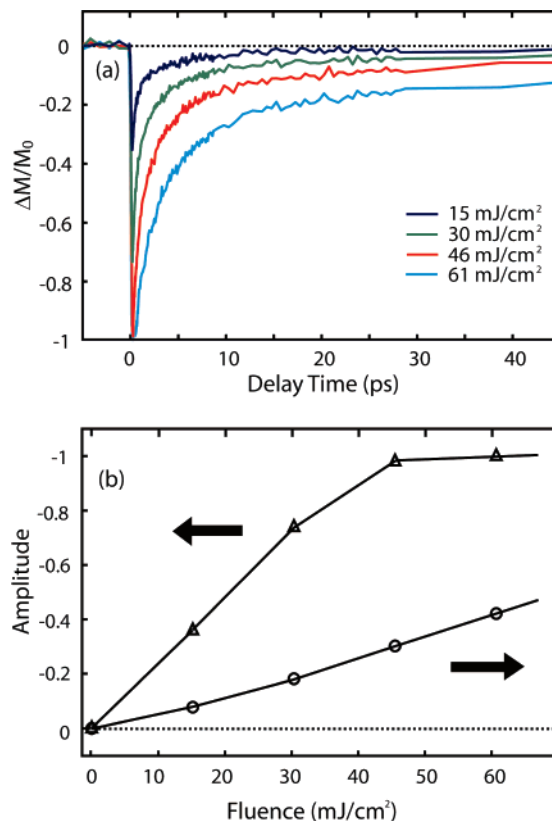
Figure 5. (a) Excitation fluence dependence of $\Delta M/M_0$ of 4.5 nm Fe_3O_4 nanocrystals. (b) Excitation fluence dependence of the amplitudes in $\Delta M/M_0$. Triangle: peak amplitude of $\Delta M/M_0$. Circle: amplitude of the exponential fit for $\tau = \sim 200$ ps recovery component. Solid lines superimposed on the marks are guides to an eye.

laxation, spin−orbit coupling during coherent excitation, magnon excitation by fast relaxing electrons or carriers, etc.[8,9,30,31] Despite the recent progresses, understanding the microscopic mechanisms of ultrafast demagnetization continues to be a challenge because the pathways allowing the flow of both the energy and spin angular momentum on the relevant time scales need to be identified.[32]

To obtain a deeper and more quantitative understanding of the dynamics of the demagnetization and its recovery, $\Delta M/M_0$ was measured at various excitation fluences. Figure 5a shows the time-dependent $\Delta M/M_0$ of 4.5 nm Fe_3O_4 nanocrystals as a function of the excitation fluence. The peak value of $\Delta M/M_0$ negatively increases with the excitation density and saturates near -1, that is, almost complete demagnetization, at the excitation fluence of 46 mJ/cm^2 corresponding to $\sim 10\%$ excitation density as shown in Figure 5b. This suggests that each absorbed photon initially destroyed the magnetic ordering in ~ 10 times larger number of metal ions for 4.5 nm Fe_3O_4 nanocrystals. A similar degree of the destruction of the magnetic ordering by the optical excitation was observed earlier in ferromagnetic chalcogenide surfaces.[29]

While their relative amplitudes vary as a function of the excitation fluence, the biphasic feature of the recovery, that is, fast ($\tau < 5$ ps) and slow ($\tau = \sim 200$ ps) phases, is maintained in the entire range of the excitation fluence of

this study. For $\tau = \sim 200$ ps component, the amplitude increases slightly superlinearly to the excitation fluence; see Figure 5b. Slight superlinearity is due to an additional contribution of the multiphoton absorption, which was also observed in the transient absorption data. (See Supporting Information) The fact that the slow magnetization recovery and transient absorption occur on comparable time scales and that they exhibit similar excitation fluence dependence suggest that slow magnetization recovery reflects the relaxation of the excited-state to the ground state. On the other hand, the fast recovery component of magnetization, carrying the larger fraction of the amplitude, does not have a corresponding feature in the transient absorption data.

To explain the distinct biphasic recovery of the magnetization, several possibilities can be considered. One explanation is the unequal recovery time scales for the surface and core magnetization of the nanocrystals. In this case, the faster and slower recovery components could be associated with the surface and the core, respectively. However, the difference of the recovery time scales is too large to explain simply by the heterogeneity of metal ion sites alone. Moreover, the surface magnetic moments are generally considered more disordered than core with a minor contribution to the total magnetization at high temperatures and low external fields, such as the present experimental condition.[20] In that case, the amplitude of the faster recovery component, ~ 10 times larger than that of the slower component in Figure 5b, cannot be easily accounted for by the disordered surface magnetic moments. The fact that the fast dynamics component is absent in the transient absorption data also suggests that it is not associated with the electronic relaxation back to the ground state and has a microscopic origin different from $\tau \approx 200$ ps component. Another possible explanation may come from the consideration of the spin−spin correlation time of magnetic moments. Because the response of the system is linked to its time autocorrelation via fluctuation− dissipation theorem in the linear response regime,[33] examining the decay of the spin−spin time correlation function will provide an insight into the dynamics of the magnetization. According to the earlier simulations on the spin−spin time correlation function, $C(t)$, for various model systems, the effective decay time constant of $C(t)$ was estimated to be in the range of a few to tens of picoseconds.[34,35] This is similar to the time scale of the faster magnetization recovery component in Figure 5a. These facts suggest that fast recovery component of $\Delta M/M_0$ reflects the partial reestablishment of the ferrimagnetic ordering before the relaxation of the electrons, while $\tau = \sim 200$ ps component reflects the additional recovery of the magnetic ordering accompanying the electronic relaxation.

To obtain a further insight into the magnetization dynamics and their dependence on the size of the nanocrystals, $\Delta M/M_0$ was measured for Fe_3O_4 nanocrystals of three different sizes. Figure 6a compares $\Delta M/M_0$ of 4.5, 7.5, and 10 nm Fe_3O_4 nanocrystals. The excitation density and the optical density at the probe wavelength were kept nearly the same for all three samples for this comparison. $\Delta M/M_0$ exhibits a strong dependence on the size of the nanocrystal, especially
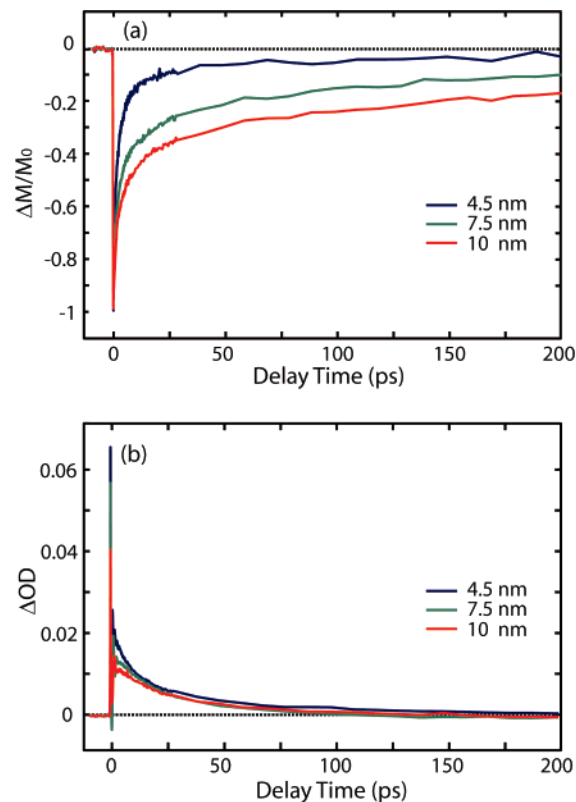
Figure 6. Size-dependent $\Delta M/M_0$ (a) and ΔOD (b) of Fe_3O_4 nanocrystals at the excitation fluence of 46 mJ/cm^2. The amplitude of slower recovery component of $\Delta M/M_0$ increases with the size of the nanocrystal while ΔOD exhibits no strong size-dependence.

for its amplitude, while the biphasic recovery is observed for all the sizes. This is in contrast to the transient absorption data shown in Figure 6b, which do not exhibit significant size-dependent dynamics except at very early delay times. For the fast recovery component of $\Delta M/M_0$, its relative contribution to the overall recovery dynamics becomes smaller as the size of the nanocrystal increases. On the other hand, the amplitude of the slow recovery component increases significantly with the size. The time scales of the magnetization recovery exhibit a slight increase as the size of the nanocrystal increases; 3−7 and 200−360 ps for the fast and slow recovery component, respectively.

The increase of the amplitude for the slow recovery component of $\Delta M/M_0$ with the size of the nanocrystals indicates that photoexcitation has a stronger influence on the destruction and recovery of the magnetic ordering for the larger nanocrystals. Size-dependent lattice temperature due to different cooling rate, which is in quasi-equilibrium with the spin degrees of freedom, cannot explain the above size-dependence. The temperature increase in the lattice is estimated to be less than 100 K under the present experimental condition during the first several picoseconds from the temperature-dependent coherent acoustic phonon frequency and temperature-dependent elastic moduli of typical ferrite materials.[36,37] Langevin function describing the temperature and field dependence of the magnetization of superparamagnetic particles predicts $\Delta M/M_0$ should not be affected by more than a few percent for 7.5 and 10 nm nanocrystals.[38,39] One way to explain this observation is by

invoking the size-dependent magnetic ordering within the nanocrystal. One could argue that the destruction and recovery of the ferrimagnetic ordering by the photoexcitation would be more pronounced if the correlation among magnetic moments of Fe ions was stronger. In this case, the observed size dependence of $\Delta M/M_0$ would indicate that the magnetic moments have a higher degree of correlation or stronger ordering within the nanocrystal as the size increases. In fact, the finite-size effect on the magnetic ordering in nanocrystals has been an important issue, together with other size-dependent properties such as the static magnetization, magnetic phase transition temperature, and superparamagnetic relaxation.[38,40,41] However, understanding of the size-dependent magnetic ordering is still somewhat controversial. Many experimental studies on the magnetic ordering of the magnetic nanocrystals employed Mössbauer spectroscopy or X-ray magnetic circular dichroism, which measured the average spin-canting angles. While these studies revealed that the smaller nanocrystals exhibit the larger average spin canting, that is, the larger average spin disorder, the interpretation was unequivocal. It could be explained with either the core/shell model involving the disordered surface and the ordered core[42,43] or the model assuming a more homogeneous size-dependent ordering throughout the whole volume.[44,45]

The dichotomic core/shell model is, however, incompatible with our experimental observation of the size-dependent $\Delta M/M_0$. Because both ΔM and M_0 should have the size dependence from the same origin, that is, the disordered surface, $\Delta M/M_0$ should not exhibit a pronounced size dependence. The size-dependent magnetic ordering throughout the whole volume of the nanocrystals is consistent with the observed size-dependence of $\Delta M/M_0$ in this study. The increase of the faster recovery time scale of $\Delta M/M_0$ with the size of the nanocrystals can also be understood in terms of the size-dependent magnetic ordering throughout the volume. Because we associated the faster magnetization recovery component with the partial reestablishment of the magnetic ordering, whose dynamics are dictated by $C(t)$, the longer time constant for the larger nanocrystal may reflect the stronger spin correlation within the nanocrystal.[34,35]

In summary, we have investigated the ultrafast dynamics of the demagnetization and the recovery of the magnetization following the photoexcitation of Fe_3O_4 nanocrystals. The dynamics of the slowly recovering component of $\Delta M/M_0$ were well correlated with the dynamics of electronic relaxation, while the faster recovery component was assigned to the partial reestablishment of the ferrimagnetic ordering before the electronic relaxation. The amplitude of $\Delta M/M_0$ was strongly dependent on the size of the nanocrystals, suggesting the size-dependent magnetic ordering within the nanocrystal.

Supporting Information Available: Probe wavelength dependence of ΔOD, excitation fluence dependence of ΔOD, and probe wavelength dependence of $\Delta M/M_0$ of Fe_3O_4 nanocrystals. This material is available free of charge via the Internet at http://pubs.acs.org.

References

(1) Zhang, G.; Hübner, W.; Eric, B.; Bigot, J.-Y. *Top. Appl. Phys.* **2002**, *83*, 245.

(2) Wang, J. G.; Sun, C. J.; Hashimoto, Y.; Kono, J.; Khodaparast, G. A.; Cywinski, L.; Sham, L. J.; Sanders, G. D.; Stanton, C. J.; Munekata, H. *J. Phys.: Condens. Matter* **2006**, *18*, R501.

(3) Beaurepaire, E.; Merle, J. C.; Daunois, A.; Bigot, J. Y. *Phys. Rev. Lett.* **1996**, *76*, 4250.

(4) Rhie, H. S.; Durr, H. A.; Eberhardt, W. *Phys. Rev. Lett.* **2003**, *90*, 247201.

(5) Melnikov, A.; Radu, I.; Bovensiepen, U.; Krupin, O.; Starke, K.; Matthias, E.; Wolf, M. *Phys. Rev. Lett.* **2003**, *91*, 227403.

(6) Ju, G. P.; Hohlfeld, J.; Bergman, B.; van de Veerdonk, R. J. M.; Mryasov, O. N.; Kim, J. Y.; Wu, X. W.; Weller, D.; Koopmans, B. *Phys. Rev. Lett.* **2004**, *93*, 197403.

(7) Wang, J.; Sun, C.; Kono, J.; Oiwa, A.; Munekata, H.; Cywinski, L.; Sham, L. J. *Phys. Rev. Lett.* **2005**, *95*, 167401.

(8) Stamm, C.; Kachel, T.; Pontius, N.; Mitzner, R.; Quast, T.; Holldack, K.; Khan, S.; Lupulescu, C.; Aziz, E. F.; Wietstruk, M.; Durr, H. A.; Eberhardt, W. *Nat. Mater.* **2007**, *6*, 740.

(9) Zhang, G. P.; Hübner, W. *Phys. Rev. Lett.* **2000**, *85*, 3025.

(10) Koopmans, B.; Ruigrok, J. J. M.; Longa, F. D.; de Jonge, W. J. M. *Phys. Rev. Lett.* **2005**, *95*, 267207.

(11) Kimel, A. V.; Kirilyuk, A.; Usachev, P. A.; Pisarev, R. V.; Balbashov, A. M.; Rasing, T. *Nature* **2005**, *435*, 655.

(12) Wolf, S. A.; Awschalom, D. D.; Buhrman, R. A.; Daughton, J. M.; von Molnar, S.; Roukes, M. L.; Chtchelkanova, A. Y.; Treger, D. M. *Science* **2001**, *294*, 1488.

(13) Prinz, G. A. *Science* **1998**, *282*, 1660.

(14) *Spin Dynamics in Confined Magnetic Structures II*; Springer: Berlin 2003; Vol. 87.

(15) Andrade, L. H. F.; Laraoui, A.; Vomir, M.; Muller, D.; Stoquert, J. P.; Estournes, C.; Beaurepaire, E.; Bigot, J. Y. *Phys. Rev. Lett.* **2006**, *97*, 127401.

(16) Buchanan, K. S.; Zhu, X. B.; Meldrum, A.; Freeman, M. R. *Nano Lett.* **2005**, *5*, 383.

(17) Klimov, V. I.; Mikhailovsky, A. A.; McBranch, D. W.; Leatherdale, C. A.; Bawendi, M. G. *Science* **2000**, *287*, 1011.

(18) Scholes, G. D.; Kim, J.; Wong, C. Y.; Huxter, V. M.; Nair, P. S.; Fritz, K. P.; Kumar, S. *Nano Lett.* **2006**, *6*, 1765.

(19) Sun, S.; Zeng, H. *J. Am. Chem. Soc.* **2002**, *124*, 8204.

(20) Goya, G. F.; Berquó, T. S.; Fonseca, F. C.; Morales, M. P. *J. Appl. Phys.* **2003**, *94*, 3520.

(21) Fontijn, W. F. J.; van der Zaag, P. J.; Devillers, M. A. C.; Brabers, V. A. M.; Metselaar, R. *Phys. Rev. B* **1997**, *56*, 5432.

(22) Dormann, J. L.; Spinu, L.; Tronc, E.; Jolivet, J. P.; Lucari, F.; D'Orazio, F. *J. Magn. Magn. Mater.* **1998**, *183*, L255.

(23) Lifshitz, E. M.; Landau, L. D.; Pitaevskii, L. P. *Electrodynamics of Continuous Media*; Pergamon Press: New York, 1984.

(24) Baumberg, J. J.; Awschalom, D. D.; Samarth, N. *J. Appl. Phys.* **1994**, *75*, 6199.

(25) Gupta, J. A.; Knobel, R.; Samarth, N.; Awschalom, D. D. *Science* **2001**, *292*, 2458.

(26) Kise, T.; Ogasawara, T.; Ashida, M.; Tomioka, Y.; Tokura, Y.; Kuwata-Gonokami, M. *Phys. Rev. Lett.* **2000**, *85*, 1986.

(27) Zvezdin, A. K.; Kotov, V. A. *Modern Magnetooptics and Magneto-optical Materials*; Taylor & Francis Group: New York, 1997.

(28) Hansteen, F.; Kimel, A.; Kirilyuk, A.; Rasing, T. *Phys. Rev. Lett.* **2005**, *95*, 047402.

(29) Ogasawara, T.; Ohgushi, K.; Tomioka, Y.; Takahashi, K. S.; Okamoto, H.; Kawasaki, M.; Tokura, Y. *Phys. Rev. Lett.* **2005**, *94*, 087202.

(30) Scholl, A.; Baumgarten, L.; Jacquemin, R.; Eberhardt, W. *Phys. Rev. Lett.* **1997**, *79*, 5146.

(31) Koopmans, B.; van Kampen, M.; Kohlhepp, J. T.; de Jonge, W. J. M. *Phys. Rev. Lett.* **2000**, *85*, 844.

(32) Stamm, C.; Tudosa, I.; Siegmann, H. C.; Stohr, J.; Dobin, A. Y.; Woltersdorf, G.; Heinrich, B.; Vaterlaus, A. *Phys. Rev. Lett.* **2005**, *94*, 197603.

(33) Kubo, R. *Rep. Progr. Phys.* **1966**, *29*, 255.

(34) Lee, J. D. *Phys. Rev. B* **2004**, *70*, 174450.

(35) Davis, S.; Gutierrez, G. *Physica B* **2005**, *355*, 1.

(36) Unpublished results. The estimation of the lattice temperature is made from ∼1% decrease of the coherent acoustic phonon frequency, which is expected for ∼100 K increase of the lattice temperature according to the data in ref 37.

(37) Antao, S. M.; Jackson, I.; Li, B.; Kung, J.; Chen, J.; Hassan, I.; Liebermann, R. C.; Parise, J. B. *Phys. Chem. Miner.* **2007**, *34*, 345.

(38) Batlle, X.; Labarta, A. *J. Phys. D: Appl. Phys.* **2002**, *35*, R15.

(39) Using Langevin function with bulk saturation magnetization of 84 emu/g, magnetic field of 0.35 T and temperature change of 100 K, changes in magnetization by 2 and 4% were predicted for 10 and 7.5 nm nanocrystal respectively.

(40) Song, Q.; Zhang, Z. J. *J. Phys. Chem. B* **2006**, *110*, 11205.

(41) Tang, Z. X.; Sorensen, C. M.; Klabunde, K. J.; Hadjipanayis, G. C. *Phys. Rev. Lett.* **1991**, *67*, 3602.

(42) Coey, J. M. D. *Phys. Rev. Lett.* **1971**, *27*, 1140.

(43) Haneda, K.; Kojima, H.; Morrish, A. H.; Picone, P. J.; Wakai, K. *J. Appl. Phys.* **1982**, *53*, 2686.

(44) Kodama, R. H.; Makhlouf, S. A.; Berkowitz, A. E. *Phys. Rev. Lett.* **1997**, *79*, 1393.

(45) Morales, M. P.; Serna, C. J.; Bodker, F.; Mørup, S. *J. Phys.: Condens. Matter* **1997**, *9*, 5461.